Received: 11 February 2023 | Revised: 3 August 2023 | Accepted: 28 August 2023

IET Generation, Transmission & Distribution

DOI: 10.1049/gtd2.12976

The Institution of Engineering and Technology WILEY

ORIGINAL RESEARCH

A robust fusion bus frequency estimation method to improve frequency oscillation damping in power systems

Ali Farahani[1] | **Amir H. Abolmasoumi**[1,2] | **Lamine Mili**[3] | **Mohammad Bayat**[1,2]

[1]Department of Electrical Engineering Arak University, Arak, Iran

[2]Research Institute of Renewable Energy, Arak University, Arak, Iran

[3]Department of Electrical and Computer Engineering Virginia Polytechnic Institute and State University, Falls Church, VA, USA

Correspondence
Amir H. Abolmasoumi, Research Institute of Renewable Energy, Arak University, Arak, 38156-8-8349, Iran.
Email: a.abolmasoumi@gmail.com, a-abolmasoumi@araku.ac.ir

Abstract

This paper proposes a new robust method for accurately and reliably estimating remote bus frequencies in a power system. Two different measurement sources for the remote bus frequency are considered, that is, the ideal Frequency Divider (FD) and the Synchronous Reference Frame Phase Locked Loops (SRF-PLLs). Each measurement signal encounters different uncertainties and data quality issues. In this paper, both data sources are employed and fused together to better estimate the remote bus frequencies. To this end, the model structure of the power system is selected and an Unscented Kalman Filter (UKF) is utilized together with a fusion covariance intersection method to enhance the accuracy of the estimated bus frequency. Since the fusion estimation method fails in case of quality issues on both channels, a robust Generalized Maximum-likelihood UKF (GM-UKF) using a novel outlier detection criteria is developed. The impact of the resulting robust fusion filter on the estimation of the remote bus frequencies and on the performance of WAPSS, which makes use of the estimated frequencies as the feedback signal, is examined via simulations. The results demonstrate the excellent performance and reliability of the proposed method in dealing with noise filtering and outlier suppression while ensuring a high statistical efficiency.

1 | INTRODUCTION

The damping of frequency oscillations is of essential importance for guaranteeing the stability of wide-area power systems with inter-connected synchronous generators. Dominant low frequency oscillations include local modes in the range of 1–2 Hz and, more importantly, inter-area modes in the range of 0.1–1 Hz [1, 2]. If not damped efficiently, these modes may result in line and generator outages, power system splitting into islands, and cascading failures leading to large-scale blackouts [3]. The common solution for the stabilization of the power systems is to deploy local Power System Stabilizers (PSSs) [2, 4] and Flexible AC Transmission System (FACTS) devices [5, 6]. As for the local PSSs, they use the local frequency measurements as feedback signals sent to the voltage automatic regulators to stabilize the inter-area electromechanical oscillations [2]. However, the local stabilizers are shown not the best option to achieve this goal. Indeed, inter-area oscillations, which are observable at buses belonging to different areas, should be damped by stabilizers measuring frequencies in one area and acting on generators in another area [4, 7]. In other words, Wide-Area Power System Stabilizers (WAPSSs) that take the frequency of a bus in different area as the measurement feedback are the right option [4, 8–10].

The essential step in all design methods of a WAPSS is to determine the optimal bus on which the feedback frequency should be measured and the generator at another area where the WAPSS should be placed. A large number of studies in the literature deal with the placement of the meters and WAPSSs to achieve the highest system observability and controllability based on a sensitivity analysis [11], a geometric-based approach [12], and wide-area damping controllers [9]. There are also several WAPSS design schemes proposed in the literature; see for example [7, 8] and [13]. The control scheme being considered consists of remote metered values taken from Wide-Area Measurement Systems (WAMSs), using Phasor Measurement Units (PMUs), and transmitted to a WAPSS [14]. However, providing a high quality frequency measurement from a remote bus to the

WAPSS is problematic because of the issues regarding the data quality such as uncertainties, noises and deviant data, termed outliers. The latter may be due to imperfect measuring methods or devices, sampling and processing issues, communication problems or even cyber-attacks, to name a few [15].

Regarding the frequency estimation, it is a sub-topic of the overall power system state estimation problem. There are a number of power system dynamic state estimation methods making use of the PMU measurements proposed in the literature; see for example [16, 17] and the references therein. In [18], a switched dynamic state estimation is utilized to address the problem of denial-of-service cyber attacks in power systems. Two subsystems are employed and the estimation outcomes are combined. Huang et al. [19] propose a decentralized UKF method based on the analog voltage and current measurements installed at transformer buses. Here, the magnitude and the frequency of the voltages and currents are obtained based on statistical signal processing techniques without the need of PMUs. Another method to estimate the frequency from measurements is presented in [20] using an adaptive detection methodology, which is shown to be robust to the changes in the noise statistics and the step changes in the voltage and current amplitudes and phases. In [21], a frequency estimator is designed based on the measurements by the Hilbert-transform PLLs together with a complex mean squared estimation method. Instead of using bus frequencies measured from locally installed devices such as instrument transformers or PLLs, Milano and Ortega [22] propose the FD formula to obtain the remote bus frequencies given the angular velocity of the generators since the PMUs are usually installed at the generator buses. However, the FD relies on the PMU-based rotor speed signals, which may be noisy and biased. Also the FD makes use of the susceptance matrix of the power system, whose parameters may be subjected to uncertainties. Zhao et al. [23] advocate the use of a GM-UKF aimed at robustly estimating the rotor speed, and thereby the remote bus frequency via the FD, while achieving lower communication load by transmitting only the rotor angle and speed signals to the FD calculation center. However, the locally estimated frequencies have to be transmitted through the communication channel to the FD center where the load bus frequencies are calculated. Obviously, this may introduce new errors to the transmitted signals, including missing data, various noises, and gross errors as a result of cyber-attacks or channel interference. On the other hand, different types of PLLs have been recently utilized to provide the bus frequencies [24]. As one of the best performing variants, the synchronous reference frame PLLs (SRF-PLLs) [25] are well-functioning high-bandwidth algorithms that are capable of providing a fast and accurate phase-angle estimation. In [4], the dynamic performance of the WAPSSs using either an ideal FD-calculated frequency or SRF-PLLs-based measurements are compared and the effect of the time-delays on the performance of the WAPSS are investigated.

There are several quality issues of the values provided by local bus frequency meters such as SRF-PLLs or the FD-calculated ones achieved from PMUs installed at generator buses. However, as indicated in [23, 26], PMUs may be corrupted by gross errors, communication losses, and injected false values. As for the measurement errors, they are shown to have some influence on the frequency regulators, which may be significant for large errors [27]. Huang *et al*. [28, 29] categorize the PMU quality issues such as time synchronization accuracy, data losses, and data latency and discuss each one separately. For more on the PMU measurement quality issues, see [30, 31] and the references therein for further details. Regarding the PLLs, they may be unable to guarantee low noise and high-speed response at the same time while suffering from numerical integration errors [4, 32]. Furthermore, their performance may deteriorate as a result of a step change in the speed and the presence of harmonics and unbalanced power systems [23, 32].

It is known that for large disturbances, the FD calculations provide more reliable data on remote bus frequencies compared to the SRF-PLLs. However, there are many scenarios where the SRF-PLLs measurement data contain usable data that must not be thrown away. Moreover, the FD needs the power system parameter values, which may not be available with a high precision. As a result, there are cases where the FD calculations are also unreliable to some extent. Furthermore, as discussed, some data sets transmitted over both the FD and the SRF-PLLs channels may suffer from quality issues. These weaknesses motivate us to employ both measurement sources at the same time to improve bus frequency estimation. In this paper, we investigate the fusion of two measurement feedback signals taken from the FD calculations and the SRF-PLLs to obtain more accurate and reliable estimates from of the frequency at the remote bus and, as a result, to enhance the overall efficiency of the WAPSS. The current paper may be seen as the extension of the results in [23] into the case where SRF-PLLs measurements are available. To perform the fusion, we first make use of a covariance intersection method in combination with the UKF method, which we call fusion UKF. The latter takes the measurements from the FD and the SRF-PLLs and calculates the dynamically weighted sum of these measurements to construct the feedback signal for the WAPSS. Since two measurement signals come from different sources, they may suffer from different data quality issues. Consequently, the fusion filter is used to preserve the quality of the output feedback signal in presence of uncertainties, noises, and outliers in one of the channels. The fusion will be shown to be the most effective method when one channel is contaminated with large errors.

To robustify the fusion filter against outliers or thick-tailed non-Gaussian noises, which may occur simultaneously at both measurements channels, we suggest to utilize the robust GM-UKF recently presented in [33–37] as a powerful power system dynamic state estimator. The GM-UKF makes use of the concept of projection statistics to weight the data based on their inlier-outlier behaviour. As an extension to the fusion estimation, the outlier detection step in the GM-UKF is modified. Specifically, the organization of the data vector set for which the projection statistics and the corresponding outlier weights that are calculated are modified to achieve a fusion GM-UKF. It is verified that in addition to the general advantages of the fusion method, it also enhances the outlier

detection capability of the robust estimation process presented in [23] and accordingly improves the performance of the robust frequency estimation by the GM-UKF. In other words, the fusion GM-UKF proposed in this paper is more robust than the GM-UKF presented in [23]. We also show that especial attention should be paid to choosing the appropriate dynamic model of the power system in terms of its relationship with system observability and its communication load. The latter is determined by the number of metered signals (for example electrical power, rotor speed etc.) that are sent through the communication channels to the estimation center. This work is the generalization of the initial ideas in [38, 39] by the authors of the present paper.

The proposed fusion UKF and fusion GM-UKF methods are simulated on two cases. The two-area four-machine power system [4] and the New England 39-bus 10-machine power system *NEW England Case System* [9]. The results show the improvement of the bus frequency estimation, which leads to better frequency oscillation damping by the PSSs in comparison with the case where the conventional FD or PLLs measurements are individually used to construct the feedback signals. It is also demonstrated that the designed fusion GM-UKF is robust to gross errors among the measurement data, which enhances the performance of the proposed method.

The next sections of the paper are organized in the following manner: Section 2 presents preliminaries to power system stabilization and WAPSS structure, and explain how to obtain the frequency at the target point via the SRF-PLLs and the FD methods. Section 3 discusses the architecture of the proposed state estimation method. Section 4 proposes the GM-UKF to robustify the fusion filter. Section 5 provides some simulations carried out on the New England 10-machine system and analyzes the performance of the proposed state estimation method in various scenarios. Finally Section 6 concludes the paper.

2 | PRELIMINARIES TO WIDE-AREA POWER SYSTEM STABILIZER AND FREQUENCY MEASUREMENTS

The algebraic differential state-space equations that governs a power system are expressed as

$$\begin{aligned} \dot{\boldsymbol{x}} &= \tilde{\boldsymbol{f}}(\boldsymbol{x},\boldsymbol{y},\boldsymbol{u}), \\ \mathbf{g}(\boldsymbol{x},\boldsymbol{y},\boldsymbol{u}) &= 0, \end{aligned} \tag{1}$$

where $\tilde{\boldsymbol{f}}$ and $\mathbf{g}$ are the vector functions of the power system state vector $\boldsymbol{x}$, the dependent variables contained in $\boldsymbol{y}$, and the control input $\boldsymbol{u}$, which here is the voltage applied to the exciter of the target generator as the wide area power system stabilizer. In state estimation, some signals such as the electrical or the mechanical power are assumed to be known, resulting in a reduced dimension of $\boldsymbol{x}$ and in a larger number of input variables.

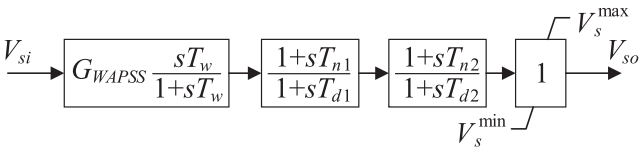

FIGURE 1 The block diagram of a power system stabilizer.

2.1 | Wide area power system stabilizer

The block diagram of the PSS is depicted in Figure 1. As observed, the PSS takes $V_{sij} = \Delta\omega$ as the feedback and applies the voltage V_{so} as an added signal to the Automatic Voltage Regulator (AVR) reference input to make change on the generator exciter on which the WAPSS is installed. The PSS is composed of a washout filter followed by the lead-lag blocks. In Figure 1, G_{WAPSS} represents the WAPSS gain, T_W is the time constant of the washout filter, and $T_{n1}, T_{n2}, T_{d1}, T_{d2}$ are the four time constants that belong to each of four stabilizing blocks. The results from [40–42] show that the inter-area oscillations are better observable when using the difference between the rotor speeds of some machines and the frequencies on some load buses in other areas of the power system. Assuming that the power system stabilizer is installed at Bus j, we get $V_{si} = \Delta\omega_{ij} = \omega_{Bi} - \omega_{Gj}$. Here, $V_{si} = \Delta\omega_{ij}$ is the feedback error signal that is fed to the PSS controller. Note that the selection of Buses i and j are based on some controllability/observability analysis based on, for example, the geometric approach [4]. Calculating the feedback signal V_{si} calls for two elements to be known, namely ω_{Bi} and ω_{Gj}. Therefore, the generator rotor speed and the bus frequency are essential components in the construction of the feedback signal. Accordingly, improving the estimation of the bus frequency contributes to improve the performance of the frequency oscillation control. As mentioned before, the output of the PSS block V_{so} is an added control voltage to the reference voltage of the local AVR,(V_{ref0}), and enables the controller to damp the electromechanical oscillations through the excitation controller. Finally, the voltage reference is then calculated as $V_{ref} = V_{ref0} + V_{so}$.

2.2 | Obtaining the value of the bus frequency

Two methods aimed at obtaining the value of the frequency on the remote buses are considered. The first method consists in measuring the frequency by using the SRF-PLLs as a frequency measurement device installed at a local bus. The PLLs devices are primary aimed at synchronizing the power electronic converters to the electrical grid. A byproduct is the estimation of the deviation of the frequency from its base value [32]. The input is the three-phase bus voltage. The voltages are transformed to the $d-q$ reference frame and the q component is controlled to track zero value, which guarantees that the converter is complete synchrony with the AC power system frequency at the connection point and utilizes $v_d(t)$ as the phase reference. Note that if the locked angle, θ, is the same as the angle of the system voltage $v_{abc}(t)$, then the Park transformation requires that $v_q(t)$

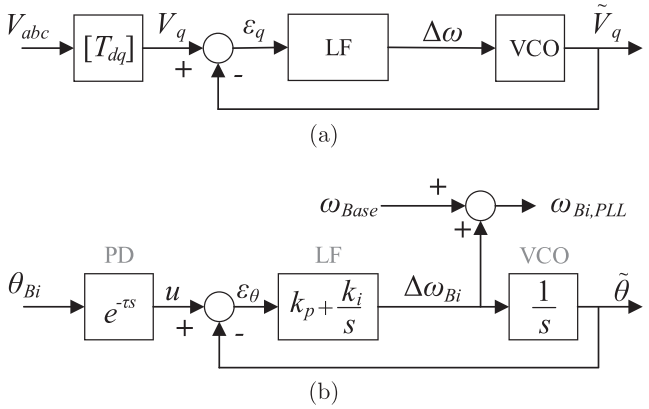

FIGURE 2 The structure of the SRF-PLL: (a) the overall idea of SRF-PLL, and (b) the frequency estimation by SRF-PLL.

is equal to zero and $v_d(t)$ is constant. Figure 2a represents the idea of SRF-PLLs, where V_{abc} denotes the three-phase voltages at the bus of connection. Also V_d and V_q denote the dq voltages. Accordingly, $[\mathbf{T}_{dq}]$ is the transfer matrix to the dq reference frame and θ_{Bi} is the bus angle. As shown in Figure 2, a Proportional Integral (PI) controller and an integrator are used as the Loop Frequency (LF) and the Voltage Controlled Oscillator (VCO), respectively. The frequency of the local bus is obtained via $\omega_{Bi} = \omega_{Base} + \Delta\omega_{Bi}$, where ω_{Base} denotes the base frequency of the power system. Since the measurement of the signal and the application of the Park transformation is not instantaneous, it is modeled by a time delay. Moreover, as seen in Figure 2, it is possible to extract an estimation of the frequency deviation from the SRF-PLLs. Here, it is assumed that the frequency measurement by the SRF-PLLs is precise. However, there are some reported drawbacks such as the tradeoff between the noise and the response speed, the numerical integration errors, and the vulnerability to step changes in the speed [4, 32]. There may also additional vulnerabilities to harmonics and power system unbalance [23, 32]. By defining

$$x_1 = \tilde{\theta}, x_2 = \int \varepsilon_\theta \, dt, \tag{2}$$

the SRF-PLLs will be described by the following dynamic state-space equations:

$$\begin{aligned} \dot{x_1} &= -k_p x_1 + k_i x_2 + k_p u, \\ \dot{x_2} &= -x_1 + u. \end{aligned} \tag{3}$$

The frequency value is then calculated as

$$y_{PLL} = \omega_{Bi,PLL} = -k_p x_1 + k_i x_2 + k_p u + \omega_{Base}. \tag{4}$$

The measurements are sent to the WAPSS or a processing center through a communication network, which may impose further quality issues such as different noises, missing data, and gross errors.

Another method for calculating the frequency of the local target bus makes use of the FD formula proposed by [22]. According to FD method, the bus frequencies can be calculated from the known generator rotor speeds as follows:

$$\begin{aligned} \Delta\boldsymbol{\omega}_B &= \mathbf{D}\Delta\boldsymbol{\omega}_G, \\ \mathbf{D} &= -(\mathbf{B}_{BB} + \mathbf{B}_{B0})^{-1}\mathbf{B}_{BG}, \\ \Delta\omega_{Bi,FD} &= \mathbf{d}_i\Delta\boldsymbol{\omega}_G. \end{aligned} \tag{5}$$

Here the vectors $\Delta\boldsymbol{\omega}_B$ and $\Delta\boldsymbol{\omega}_G$ are the deviations of the bus frequencies and generator speeds from their base values; the matrices $\mathbf{B}_{BB}$, $\mathbf{B}_{B0}$, and $\mathbf{B}_{BG}$ are the susceptance matrices of the power transmission system, and $\mathbf{d}_i$ is the i-th row of the matrix $\boldsymbol{D}$. The FD method has been investigated from the viewpoint of numerical stability and complexity in [23] and [43].

3 | DYNAMIC STATE ESTIMATION USING THE FUSION UKF METHOD

As discussed in Section 2, two methods can be used to calculate the value of the selected load bus frequency, that is, the FD calculations and the SRF-PLLs measurements. Each of these methods are exposed to various types of uncertainties. The SRF-PLLs measurements may be contaminated by noises and outliers. Besides, the transmission of such measurement through the communication channel may add even more uncertainties. On the other hand, the FD method also needs accurate values of the generator speeds at its inputs. However, these values should be first estimated by local decentralized estimators using PMUs. Now, these PMUs suffer from additive noise and biases. To address this problem, Zhao et al. [23] propose to use a robust FD based on a robust GM-UKF [33–36]. While this method locally deals with observation outliers among the measurements as well as structural and innovation outliers in the assumed dynamic model to avoid the deviation of the frequency estimation, it is vulnerable to gross-errors when the signals are transmitted to the FD center.

3.1 | Structure of the dynamic state estimation for WAPSS

In this paper we construct an estimation structure based on a data fusion filter to improve the feedback signal using both the FD and the SRF-PLL methods. Note that this method is robust, especially when only one of the measurements suffers from communication failure or strong noise at a certain time. The overall structure of the wide area control of the power system using the data fusion is represented in Figure 3. As seen, the Local Frequency Estimators (LFEs) estimate the rotor speed at each generator bus. Afterwards, each local estimator sends the estimated rotor speed of the corresponding generator to the FD calculation unit to achieve the frequency of the target Bus i. Such calculated frequency may be contaminated by various

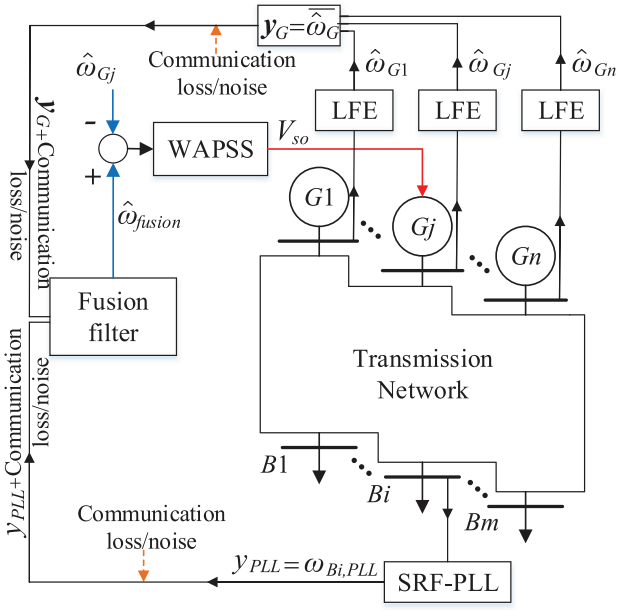

FIGURE 3 The overall structure of wide area control via WAPSS using the fusion filter to mix the frequency data from FD and SRF-PLL.

noises and gross errors as a result of processing and transmission noises or missing data. On the other hand, the frequency measurements in Bus i can be performed by the SRF-PLLs. In general, the uncertainties on frequency measurements received at the feedback center from the SRF-PLLs are different from those of the FD-calculated frequencies. The data fusion filter combines two data signals by utilizing filtering methods depending on the considered power system dynamic model. If a small signal dynamic model is considered, the fusion Kalman filter is suggested. Now, if a nonlinear model is considered, the UKF may be used as the basis estimator. However, when there are observation, innovation, or structural outliers either among the received measurement data or within the assumed power system dynamic model, the GM-UKF should be applied.

The selection of the dynamic model for the fusion filter is of critical importance. Utilizing a highly detailed dynamic model with too many states weakens the system observability, resulting in a poor performance of the frequency estimation. Alternately, employing simple models with limited number of states while considering mechanical or electrical power on each generator as known inputs will enhance the system observability and, as a result, will improve the performance of the frequency estimation. The model selection will be discussed more in the next sections.

3.2 | Fusion unscented Kalman filter

Data fusion techniques merge the measurement data from two or more sensors to obtain more accurate outcomes [44]. there are plenty of research works on measurement fusion methods as applied to dynamic systems [45]. Consider the power system nonlinear dynamical model expressed as

$$\begin{aligned} \boldsymbol{x}_{k+1} &= \boldsymbol{f}(\boldsymbol{x}_k, \boldsymbol{u}_k), \\ \boldsymbol{y}_k &= \boldsymbol{h}(\boldsymbol{x}_k) + \boldsymbol{v}_k = \boldsymbol{H}_k \boldsymbol{x}_k + \boldsymbol{v}_k. \end{aligned} \tag{6}$$

First, it is assumed that the measurement noises $\mathbf{v}_k$ on SRF-PLL measurements and also on signals received from the generator units (say the local unit rotor speeds) include only Gaussian noises as a result of being transmitted through the communication network. Later in Sections 3.4 and 3.5, this assumption is relaxed and it is assumed that there are outliers among measurements. It can be interpreted as non-Gaussian noise contamination. For example, the measurements could be contaminated with a thick-tailed noise such as Cauchy. The GM-UKF addresses this problem. The exact statistical parameters of outliers are not necessary to be known.

For the given discrete-time state space the fusion UKF calculates the estimates of the states in two steps which are referred to as the prediction and update steps. The process is carried out in a recursive manner. The UKF processes a set of $2n$ sample points, called sigma points. In the beginning of each step, sigma points are obtained as

$$\boldsymbol{X}^i_{k-1|k-1} = \hat{\boldsymbol{x}}_{k-1|k-1} \pm \left(\sqrt{nP_{k-1|k-1}}\right)_i, \quad i = 1, \ldots, n, \tag{7}$$

where $\boldsymbol{P}_{k-1|k-1}$ is the error covariance of the previous step and $\sqrt{n\boldsymbol{P}_{k-|k-1}}$ is the square-root which may come from Cholesky decomposition. Here, n is the order of the system. Sigma points propagate through the evolution equation to produce the prediction as

$$\boldsymbol{X}^i_{k|k-1} = \boldsymbol{f}\left(\boldsymbol{X}^i_{k-1|k-1}\right). \tag{8}$$

The predicted state vector and the predicted covariance matrix of estimations are given by

$$\begin{aligned} \hat{\boldsymbol{x}}_{k|k-1} &= \sum_{i=1}^{2n} \gamma_i \boldsymbol{X}^i_{k|k-1} = \boldsymbol{f}\left(\boldsymbol{X}^i_{k-1|k-1}, \boldsymbol{u}_k\right), \\ \boldsymbol{P}_{k|k-1} &= \sum_{i=1}^{2n} \gamma_i \left(\boldsymbol{X}^i_{k|k-1} - \hat{\boldsymbol{x}}_{k|k-1}\right)\left(\boldsymbol{X}^i_{k|k-1} - \hat{\boldsymbol{x}}_{k|k-1}\right)^T + \boldsymbol{Q}_k, \\ \boldsymbol{Y}_{k|k-1} &= \boldsymbol{H}_k \boldsymbol{X}_{k|k-1}, \\ \hat{\boldsymbol{y}}_{k|k-1} &= \sum_{i=1}^{2n} \gamma_i \boldsymbol{Y}_{i,k|k-1}, \end{aligned} \tag{9}$$

where $\alpha_i = 1/2n$ is the equal weight attributed to for the sigma points. After the prediction completed, the estimated states and covariance are updated step then is carried out to calculated the

as follows:

$$\begin{aligned}
\boldsymbol{P}_y &= \sum_{i=1}^{2n} \gamma_i \left(\boldsymbol{Y}^i_{k|k-1} - \hat{\boldsymbol{y}}_{k|k-1}\right)\left(\boldsymbol{Y}^i_{k|k-1} - \hat{\boldsymbol{y}}_{k|k-1}\right)^T,\\
\boldsymbol{P}_{xy} &= \sum_{i=1}^{2n} \gamma_i \left(\boldsymbol{X}^i_{k|k-1} - \hat{\boldsymbol{x}}_{k|k-1}\right)\left(\boldsymbol{Y}_{i,k|k-1} - \hat{\boldsymbol{y}}_{k|k-1}\right)^T,\\
\boldsymbol{K}_k &= \boldsymbol{P}_{xy}\boldsymbol{P}_y^{-1},\\
\hat{\boldsymbol{x}}_{k|k} &= \hat{\boldsymbol{x}}_{k|k-1} + \boldsymbol{K}_k\left(\boldsymbol{y}_k - \hat{\boldsymbol{y}}_{k|k-1}\right),\\
\boldsymbol{P}_{k|k} &= \boldsymbol{P}_{k|k-1} - \boldsymbol{K}_k \boldsymbol{P}_y \boldsymbol{K}_k{}^T,
\end{aligned} \tag{10}$$

where in (9) and (10) $\boldsymbol{y}_k = [y_{PLL,k}\, y_{G1,k} \cdots y_{Gn,k}]^T$ is vector of measurements, here the PLL frequency measurement $y_{PLL,k}$ and measured values of the generator rotor angular velocity values $[y_{G1,k} \cdots y_{Gn,k}]^T$. The matrix $\boldsymbol{H}_k = diag(\boldsymbol{H}_{PLL,k}, \boldsymbol{I}_n)$ determines the dependency of the measurements on the states. Moreover, matrices $\mathbf{Q}_k$ and $\mathbf{R}_k$ are the covariance of the process and observation noises, respectively. The FD formula utilizes the estimated generator rotor speeds to calculate the $i-th$ bus frequency as

$$\hat{\boldsymbol{y}}_{FD,k} = \hat{\omega}_{Bi,FD,k} = \boldsymbol{H}_{FD}\hat{\boldsymbol{y}}_{\boldsymbol{G,k}} = \boldsymbol{H}_{FD}\left[\hat{y}_{G1,k} \ \cdots \ \hat{y}_{Gn,k}\right]^T, \tag{11}$$

where $\boldsymbol{H}_{FD}$ is the same as $\boldsymbol{d}_i$ given by (5). Let the estimated frequency of the $i-th$ bus be calculated as $\tilde{\boldsymbol{y}}_{\boldsymbol{k}} = [\hat{y}_{PLL,k}\ \hat{y}_{FD,k}]^T$. Thus, the error covariance reduces to

$$\boldsymbol{S}_k = \mathrm{cov}\left(\tilde{\boldsymbol{y}}_k - \tilde{\boldsymbol{H}}_k\hat{\boldsymbol{x}}_{k|k}\right) = \begin{bmatrix} \alpha_k & 0 \\ 0 & \beta_k \end{bmatrix}, \tag{12}$$

where the error covariance matrix $\boldsymbol{S}_k$ is diagonal because the measurement errors of FD and PLL are assumed to be independent and $\tilde{\boldsymbol{H}}_{\boldsymbol{k}} = diag(\boldsymbol{H}_{PLL,k}, \boldsymbol{H}_{FD})$. Finally, the fusion signal is obtained as the weighted average of the estimates by the FD and PLL as:

$$\hat{\omega}_{fusion,k} = \frac{\alpha_k}{\alpha_k + \beta_k}\hat{y}_{FD,k} + \frac{\beta_k}{\alpha_k + \beta_k}\hat{y}_{PLL,k}. \tag{13}$$

Equation (13) implies that which means that the estimate with lower error is more weighted in calculation of the fusion estimates of the bus frequency. This method was first introduced in [46] and has been applied to a number of state estimation problems (see [47] and [48]). The next section discusses the tradeoff between the observability of the model states and the necessary communication load.

3.3 | Power system dynamical model, observability and communication load

Since the fusion state estimation technique is a wide-area estimation algorithm, communication load should be considered in the filter design. When the number of signals transferred through the communication channel increases, there may be some decrease of the reliability of the frequency estimation as a result of the network delays, signal corruptions, and cyber-attacks. Therefore, estimation methods involving lower required burden on the communication system are of interest. The UKF as applied to the FD calculations can utilize simple models of the power system, provided that the filter has access to some known signals. Let us consider the classical generator model given by

$$\begin{aligned}
\dot{\delta} &= \omega - \omega_0,\\
(2H/\omega_0)\dot{\omega} &= P_m - P_e - D_p(\omega - \omega_0),
\end{aligned} \tag{14}$$

in which δ denotes the rotor angle of the corresponding generator , ω denotes the angular rotor speed, H denotes the inertia constant, D_p denotes the friction/damping ratio, ω_0 denotes the base rotor speed, and P_m, P_e denote mechanical and active electrical powers, respectively. Here, the mechanical and electrical power values of each generator at every time step should be sent to the fusion center by each unit. Note that using (14) provides the acceptable level of observability to estimate the frequency of the target load bus. Instead of using (14), which requires dispatching the mechanical and electrical active power values through the communication network, one may consider a set of more detailed dynamical models such as the two-axis model or the flux decay model, which account for the dynamics of the automatic voltage regulator and/or of the turbine governor.

Figure 4 shows the structure of the UKF-FD with the application of three models. Figure 4a depicts the usage of the simple swing equation for each generator. In this case the electrical and mechanical powers are assumed as known inputs by the filter. Since the UKF-FD estimator is located in the fusion center, the instantaneous values of the electrical and mechanical power will be transmitted to the center. The observability here simply means whether the frequency estimation in the center is successful or not. Since the model is simple with only two state variables and the inputs, which are known by the estimator, are transmitted to the center, the system observability is high and the bus frequency estimation is successful. Note that it is common in the literature to consider the mechanical power to be fixed and known during the transient process [16, 23, 36]. If P_{mi}, $i = 1, .., N$ for all the generators are fixed and known by the filter, then the transmission of P_e is sufficient and model1 is the best model for the frequency estimation. In that case, the model selection can be skipped. There are cases where P_{mi} is time-varying or not a priori known by the filter. To address this problem, one option is to include the governor dynamics in the model used by the filter rather than to directly send the P_m value to the center. This has been shown in Figure 4b. In that case, the governor state variables can also be estimated, which is an additional benefit. However, as the number of the state

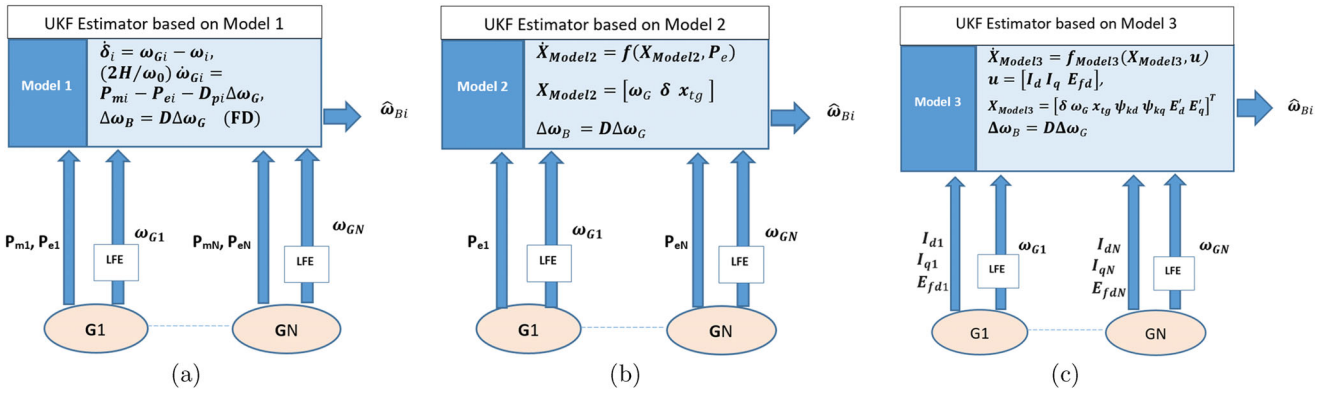

FIGURE 4 Three power system dynamical models and the required input signals for UKF-FD: (a) simple swing equation based on FD; (b) model with inclusion of the governor states; (c) complete model with inclusion of the electrical and the mechanical subsystems.

TABLE 1 Comparison of the dynamic order, observability and the communication load for three generator models used for frequency estimation from FD measurements.

	Model 1	Model 2	Model 3
Filter inputs	P_m, P_e	P_e	E_{fd}, I_d, I_q
States	ω, δ	$\omega, \delta, \mathbf{x}_{tg}$	$\omega,\delta,\psi_{kg},E'_d,\psi_{kd},E'_q,\mathbf{x}_{tg}$
Observability	High	Medium	Low
Communication load	Medium	Low	Medium

variables increases and the known values and measurements (P_e and ω_G) remain the same, the estimation procedure is of lower accuracy since the system observability decreases. As a rule of thumb, the higher the number of the model state variables are the lower the system observability will be if the number of the measured/observed signals is kept constant.

It is also possible to adopt a more complex generator model for the filter by including both the mechanical and electrical sub-systems as shown in Figure 4c. As observed, the number of the state variables of a generator is seven and the variables, I_d,I_q and E_{fd}, of each generator plus the estimated rotor speed of each generator should be transmitted to the filtering center. This results in a low system observability and, thereby, to an unsuccessful state estimation. A comparison of the required communication load and the observability level using each model can be seen in Table 1, where ω, δ, ψ_{kq}, E'_d, ψ_{kd}, E'_q are states of generator and $\mathbf{x}_{tg}$ is turbine governor state vector.

3.4 | Dealing with outliers

Taking advantage of the measurement redundancy, the UKF fusion filter is able to handle noises and uncertainties in the communication network in an effective way. This is because it makes use of the SRF-PLL measurement and the FD calculations as two independent data sets and combines them to provide accurate frequency estimation at the i-th bus. However, it makes use the fusion weighting based on the estimated covariance matrix and thereby, relies on the validity of its statistical assumptions and its accuracy. It turns out that the variance weighting may not be sufficient when there are severe deviations from the statistical assumptions. Indeed, as one of the most critical data quality issues, the measurements or calculations sent from the FD or the SRF-PLL may be contaminated by outliers. Outliers are deviant data point among measurements, which may occur in different stages of the calculation, transmission, and processing of the data. This is likely to occur when there is an overall lack of bandwidth, or partial packet dropouts, or a severe cyber-attack, or a random concurrence of outliers among the measurements.

To deal with outliers in our fusion state estimator, the samples will be first processed via an outlier detection technique. There are several techniques presented in the literature to detect and deal with outliers in power system state estimation. Among them, Projection Statistics (PS) have been shown to be robust and fast to calculate (See [49] and [50]). Using PS, different robust Kalman filters have been proposed in the literature (See [16-19] and [23]). For a sample set $\{\mathbf{z}_1, \ldots, \mathbf{z}_m\}$, PS [49] are calculated as

$$PS_i = max_{\|v\|=1} \frac{\left|\mathbf{z}_i^T \boldsymbol{v} - med_j\left(\mathbf{z}_j^T \boldsymbol{v}\right)\right|}{1.4826 med_k\left[\mathbf{z}_k^T \boldsymbol{v} - med_j\left(\mathbf{z}_j^T \boldsymbol{v}\right)\right]}, \tag{15}$$

for $i = 1, m$. PS make use of the sample median as the estimator of location and the Median-Absolute-Deviation (MAD) as the estimator of scale, which are calculated in the direction originating from the coordinate-wise medians and passing through each data points. It is shown that the squared projection statistics, PS^2, follow a χ^2_n distribution when the data points follow the Gaussian distribution [50]. In this paper, we propose to calculate the PS of the data points $\tilde{\boldsymbol{Z}}_k$ defined as

$$\tilde{\boldsymbol{Z}}_k = [\boldsymbol{Z}_{k-1}\ \boldsymbol{Z}_k], \tag{16}$$

where

$$\boldsymbol{Z}_k = \left[y_{PLL,k} - \hat{y}_{PLL,k}\, y_{G,k} - \hat{y}_{G,k}\right]^T. \tag{17}$$

It should be noted that the selection of the data points is paramount for outlier detection and weighting. Here, the

fusion framework provides the information on each generator rotor speed estimation error along with the PLL errors. By integrating all the innovation terms of the generator rotor speed estimation and of the PLL bus frequency estimation, the fusion technique constructs the $\mathbf{Z}$ matrix. More elements in $\mathbf{Z}$ lead to larger redundancy, resulting in a higher reliability of the PS. In other words, the outliers are being detected with higher probability by incorporating multiple sources of data. Also the innovations $\boldsymbol{Z}_{k-1}$ are used to get more redundancy in Step k. Then, by applying the PS, the weights are calculated as

$$w_i = \min\left(1, (d/PS_i)^2\right), \tag{18}$$

where d is chosen to be 1.5 in order to achieve high statistical efficiency under Gaussian noises.

3.5 | Generalized maximum-likelihood unscented Kalman filter

Based on the weights calculated by using The PS, the robust GM-UKF algorithm are applied to achieve a reliable estimation of the load bus frequency. Note that the GM-UKF utilizes the same steps of prediction as those of the UKF. In order to update the predictions, we first obtain the uncorrelated representation of the regression problem as follows. The UKF can be represented in a batch-mode regression as

$$\begin{bmatrix} \boldsymbol{z}_k \\ \hat{\boldsymbol{x}}_{k|k-1} \end{bmatrix} = \begin{bmatrix} \boldsymbol{H}_k \\ \boldsymbol{I} \end{bmatrix} \boldsymbol{x}_k + \begin{bmatrix} \boldsymbol{v}_k \\ \boldsymbol{e}_k \end{bmatrix}, \tag{19}$$

in which $\boldsymbol{e}_k$ is the prediction error and $\tilde{\boldsymbol{v}}_k = [\boldsymbol{v}_k\ \boldsymbol{e}_k]^T$ is the total error on the measurement and the prediction, which has a covariance matrix given by $\tilde{\boldsymbol{P}}_k = diag(\boldsymbol{R}_k, \boldsymbol{P}_{k|k-1})$, which will be factorized as $\tilde{\boldsymbol{P}} = \boldsymbol{M}_k \boldsymbol{M}_k^T$. Multiplying (19) by $\boldsymbol{M}_k^{-1}$ leads to

$$\tilde{\boldsymbol{z}}_k \overset{\Delta}{=} \boldsymbol{M}_k^{-1} \begin{bmatrix} \boldsymbol{z}_k \\ \hat{\boldsymbol{x}}_{k|k-1} \end{bmatrix} = \boldsymbol{T}_k \boldsymbol{x}_k + \tilde{\boldsymbol{v}}_k, \tag{20}$$

where $\boldsymbol{T}_k = \boldsymbol{M}_k^{-1}[\boldsymbol{H}_k\ \boldsymbol{I}]^T$ and $\tilde{\boldsymbol{v}}_k$ has the identity covariance $\boldsymbol{I}_{n+ny}$, indicating that the errors are uncorrelated. To solve for the robust Kalman gain, we make use of a Shweppe-type GM-estimator that minimizes an objective function defined as

$$J_k = \sum_{i=1}^{m+n} w_i^2 \rho(r_i), \qquad r_i = (\tilde{z}_i - a_i^T \hat{\boldsymbol{x}})/(s w_i), \tag{21}$$

where a_i^T is the i-th row of matrix $\boldsymbol{T}_k$, $s = 1.4826 b_m median|\boldsymbol{z}_i - a_i^T \hat{\boldsymbol{x}}|$ is a robust estimation of the scale and parameter b_m is a corrective coefficient. Also $\rho(.)$ is a Huber function given by

$$\rho(r_i) = \begin{cases} 0.5 r_i^2 & -\lambda < r_i < \lambda, \\ \lambda |r_i| - o.5\lambda^2 & r_i < -\lambda \ or \ r_i > \lambda, \end{cases} \tag{22}$$

where the parameter λ is the threshold between the quadratic and the linear component and is selected to be around 1.5 [50].

Putting the derivative of the objective function equal to zero results in

$$\hat{\boldsymbol{x}}_{k|k}^{(j+1)} = \left[\boldsymbol{T}_k^T \boldsymbol{Q}^{(j)} \boldsymbol{T}_k\right]^{-1} \boldsymbol{T}_k \boldsymbol{Q}^{(j)} \tilde{\boldsymbol{z}}_k, \tag{23}$$

where $\boldsymbol{Q} = diag(q(r_i))$, $q(r_i) = \varphi(r_i)/r_i$ and $\varphi(.)$ is the derivative of function $\rho(.)$ with respect to r_i. Also j represents the iteration counter. The iterations stop when $\| \hat{\boldsymbol{x}}_{k|k}^{j+1} - \hat{\boldsymbol{x}}_{k|k}^{j} \| \leq \varepsilon$, for example $\varepsilon = 0.01$. Gandhi and Mili [33] derived the influence function of this robust filter, which is shown to be bounded, and thereby its covariance matrix. After obtaining the estimation by the GM-UKF using the proposed weight calculation method, one can robustly estimate frequency on $i-th$ bus by combining the estimations obtained by two measurement sources, that is, the FD-calculated and the PLL-calculated measurements given by (13).

The whole implementation procedure of the modified fusion GM-UKF is depicted in Figure 5. Based on this figure, the local filter estimators (LFEs) transmit the needed signals of each unit (unit rotor speeds, measured powers etc) to the estimation center. The transmitted signals depends on the model in use by the central estimation algorithm. The model selection is discussed in detail in Section 3.3 of the manuscript. For generality, here, the vector of transmitted signals from the generator units is referred to as $\boldsymbol{y}_{G,k}$. The frequency measurements by the SRF-PLL are also transmitted to the estimation center. Therefore, we have two sets of measurement. Besides, the dynamic evolution models for such signals are known for the central estimators (Dynamic model of generators and SRF-PLL dynamic model). Using these known models and the received sets of measurements the estimated vector of generator speeds $\hat{\boldsymbol{y}}_{G,k}$ are calculated and is given to FD formula to calculate the frequency estimation at Bus i. The same is done for the SRF-PLL measurements. The estimates are finally combined using an covariance intersection method. Next, we show through simulations that the robust state estimation by the GM-UKF improves when the fusion of two measurements is employed.

4 | SIMULATION RESULTS

Let us firstly assess the performance of the proposed robust fusion filter when it is applied to the four machine test case [2] provided with a WAPSS. As depicted in Figure 6, each of two areas include two synchronous generators connected to step-up transformers and are related through two parallel 20-kV tie lines. To do the simulations, we make use of the power system toolbox [51]. Similar to [4], a WAPSS on Generator 3 is

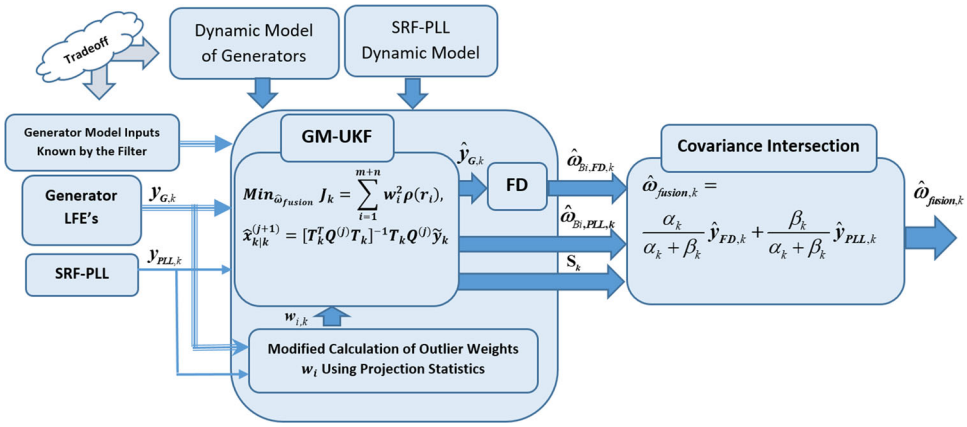

FIGURE 5 Implementation procedure of the fusion GM-UKF method for estimating the frequency at Bus *i*.

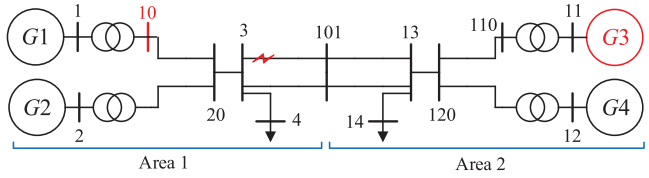

FIGURE 6 Four-machine two-area power system.

considered, taking the feedback from the remote local Bus 10. It should be noted that we make use of the same WAPSS setup and parameters used in [4, 9]. In fact, the mission here is not the WAPSS design but to provide a feedback signal of higher quality for the WAPSS. It is also assumed that the SRF-PLL is available at the same bus. A 3-phase fault is assumed to occur on the line connecting Bus 3 to 101 at time $t = 2.1$ s. The fault is removed at time $t = 2.15$ s from Bus 3 and at $t = 2.20$ s from 101. In Section 4.4, other types of faults and load shedding are also considered. To do the bus frequency estimation, local estimations of the generators' rotor speeds together with some input signals such as the generators' mechanical or electrical powers (based on the selected model) are transmitted to the fusion center, where the measurements from bus metering devices such as SRF-PLL are also received. At that center, the local estimates go through UKF filters, as we call here UKF-FD and UKF-PLL. The results are combined using the covariance weighting method. Before we evaluate the performance of the fusion filter in the frequency stabilization, we first study the effect of using different dynamic generator models on the performance of the UKF-FD filter.

4.1 | Frequency estimation results using different generator models

As we discussed previously, the selection of the model complexity level for the UKF-FD has a great impact on the observability and the required communication load. In Table 1, three models are specified, which have different levels of complexity. Model 1 consists of only the swing equations. If the electrical and mechanical power values are transmitted to the fusion filter, the UKF-FD enjoys a high level of observability despite a heavy communication load. In Model 2, the turbine-governor dynamics are taken into account by the UKF in addition to the rotor speed and rotor angle dynamics. As a result, the model is of higher order with a lower system observability. However, there is no need to transmit the mechanical power to the fusion center, which halves the communication load. The most complex Model 3 considers the dynamics of both the electrical and the mechanical subsystems. Using this model, the only signal that is known by the UKF-FD is the excitation voltage E_{fd}, which is sent to the fusion center. The system observability is low, inducing the divergence of the UKF-FD in some cases.

The performance of the UKF-FD to estimate the frequency at the load Bus 10 is assessed using the three described models. Figures 7 and 8 display the results for disturbances applied to the generator shaft torque and for the three-phase fault, respectively. While being more accurate, a system model with a higher number of states generally reduces the observability of the system. However, when using simpler models, some signals such as the generator mechanical or electrical powers may be transmitted as known inputs to the control center, yielding a higher observability with improved model accuracy. Therefore, a tradeoff between the needed number of known/transmitted signals and system's observability/accuracy leads us to choose Model 2.

4.2 | Frequency estimation results based on fusion filtering

By applying the covariance intersection method, the fusion filter combines two signals, namely one from the SRF-PLL and the other one from the FD. Under the Gaussian assumption of the noises, the output of the filter is equal to a mixture of two estimations, with higher weight placed on the one with smaller error. Although the FD calculations are more accurate than the PLL measurements, especially when large disturbances occur,

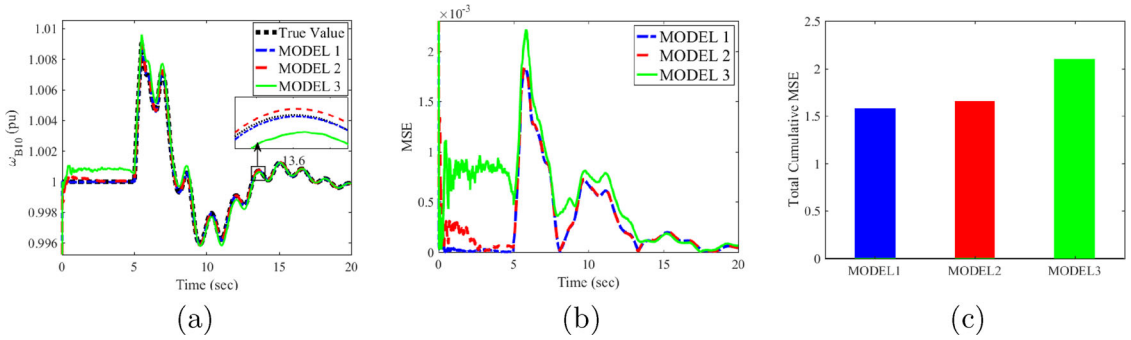

FIGURE 7 The effect of the generator dynamic model selection on the frequency estimation at Bus 10 using the UKF-FD for the torque disturbance of magnitude 0.5 p.u. applied on the generator shaft from $t = 5$ s to $t = 5.5$ s; (a) frequency estimation at the local Bus 10; (b) instantaneous frequency mean squared errors; and (c) total frequency cumulative mean squared errors.

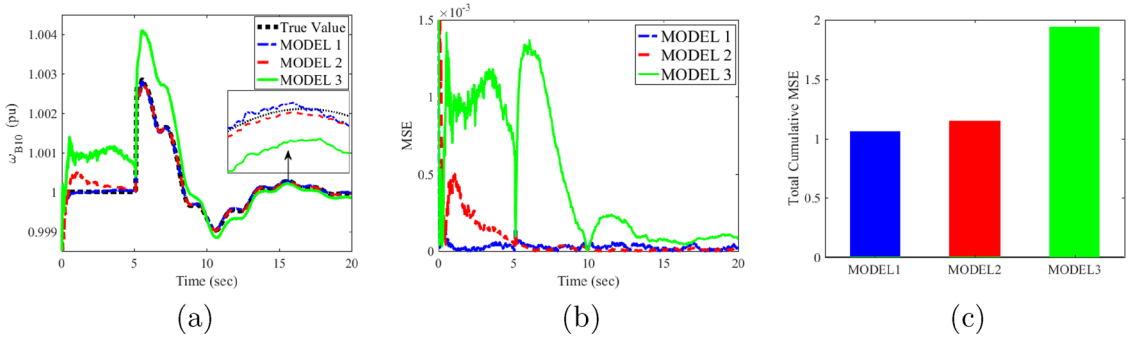

FIGURE 8 The effect of the generator dynamic model selection on the frequency estimation at Bus 10 using the UKF-FD for a three-phase fault occurred on the line between Bus 3 and 101 at $t = 2.1$ s and cleared at $t = 2.2$ s: (a) frequency estimation of the local Bus 10; (b) instantaneous frequency mean squared errors; and (c) total frequency cumulative mean squared errors.

the data received at the control center are also contaminated by several types of errors, such as communication and processing errors, to name a few. Furthermore, the FD relies on the susceptance matrix of the grid, which may include some uncertainties. Therefore, there may be situations where the communication or the process noises or other uncertainties greatly influence only one data channel while lightly impacting the other channel. In that case, the fusion process puts higher weight on the data channel that has smaller error variance, yielding more accurate final estimation results. Therefore, the fusion of the estimates improves the estimated load bus frequency, which is the feedback signal used by the WAPSS controller, and thereby enhances the quality of the frequency damping. To examine the performance of UKF fusion method, we change the noise power on both channels alternately, that is, the SRF-PLL data is becoming noisy between $t = 10$ s and $t = 12$ s and the FD measurements faces a high intensity Gaussian noise between $t = 12$ s and $t = 14$ s. Figure 9 shows that the fusion estimation provides estimates closer to the measurement with the lowest noise. Also the positive performance of the fusion method on the damping of the frequency on Generator 3 is observed. As seen, the fusion of the signals improves the feedback signal, resulting in a better damping of the oscillations as compared with each individual measurement method. Figure 9c shows a comparison of the total cumulative angular frequency deviation of the generators from the base value for the three methods of UKF-FD, UKF-PLL and UKF-Fusion from $t = 10$ s to $t = 14$ s.

4.3 | Robust frequency estimation using the fusion GM-UKF

First, recall that the suggested fusion filter is designed based on the UKF and the variance weighting method relying on the assumption of Gaussian noise. Although the fusion UKF can deal with some limited deviations from that assumption, it will be shown that the Fusion-UKF is vulnerable to noise with thick-tailed distributions such as the Cauchy distribution. It is also observed that this filter is not robust to outliers among the measurements, especially when the latter are on both measurement channels. Indeed, the outlying data points violate the Gaussian assumption and disrupt the frequency estimations provided by the fusion filter. The poor performance of the fusion method in dealing with outliers is shown in Figure 10, where the FD/SRF-PLL data are considered to be contaminated with observation outliers of magnitude 0.005 p.u, from $t = 6s$ to $t = 8s$. It is also shown that outliers can affect the frequency stabilization performed by the WAPSS.

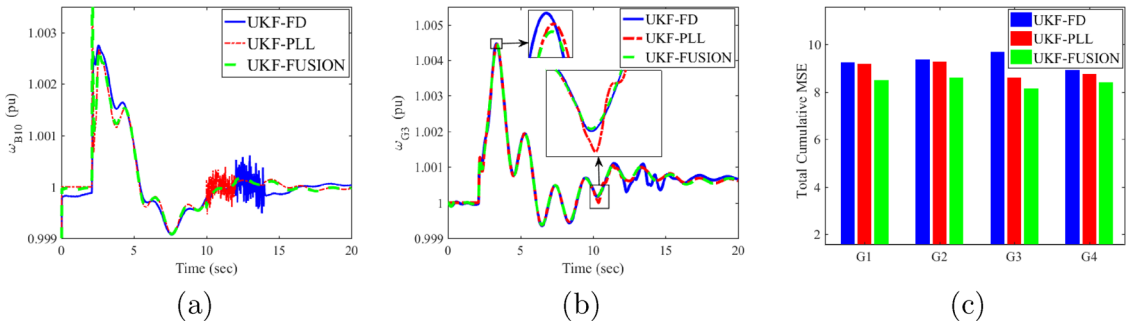

FIGURE 9 Bus frequency estimation using different fusion filters and their effect on the stabilization of the electromechanical oscillations: (a) frequency estimations of the load Bus 10; (b) the effect of the fusion filters on damping the frequency oscillations of $G3$; and (c) total frequency cumulative mean squared errors calculated from $t = 10$ s to $t = 14$ s.

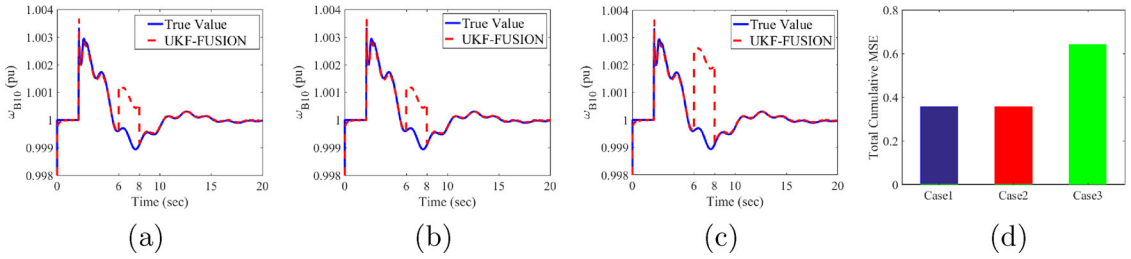

FIGURE 10 Effect of outliers on Fusion-UKF: (a) frequency estimations of the load Bus 10 when only FD measurements are contaminated with outliers of magnitude 0.005 p.u. from $t = 6$ s to $t = 8$ s (Case 1); (b) frequency estimations of the load Bus 10 when only SRF-PLL measurements are contaminated with outliers of magnitude 0.005 p.u. from $t = 6$ s to $t = 8$ s (Case 2); (c) frequency estimations of the load Bus 10 when both FD and SRF-PLL measurements are contaminated with outliers of magnitude 0.005 p.u. from $t = 6$ s to $t = 8$ s (Case 3); and (d) total frequency cumulative mean squared errors.

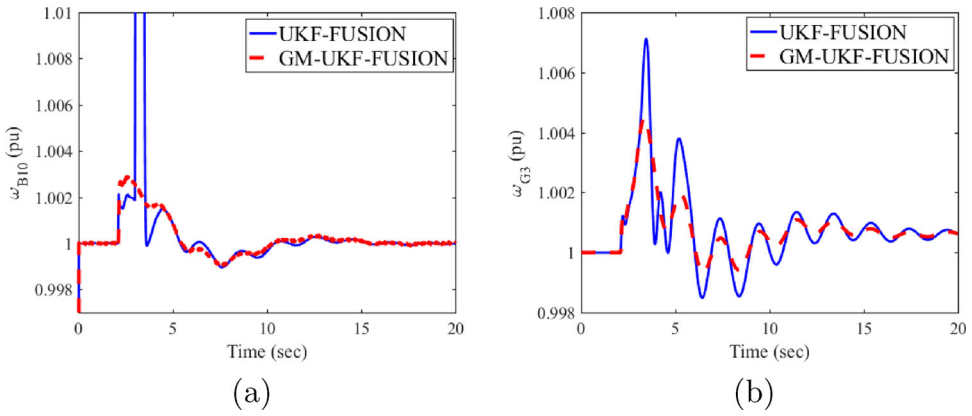

FIGURE 11 Estimation of the load bus frequency by the Fusion-UKF and the fusion GM-UKF in the presence of outliers among SRF-PLL data from $t = 3$ s to $t = 3.49$ s and among FD data from $t = 3.5$ s to $t = 4$ s using the Fusion-UKF and the fusion GM-UKF: (a) Performance of fusion UKF methods in the presence of outliers, (b) comparison of fusion UKF and fusion GM-UKF in stabilizing the frequency of Generator $G3$ in the presence of outliers.

Let us now demonstrate that using the fusion GM-UKF results in a robust estimation method. Recall that the fusion GM-UKF is a combination of the GM-UKF developed in [33–37] and the covariance intersection fusion method while making use of the weights calculated by the projection statistics. The frequency estimation by the fusion GM-UKF is compared to that of the fusion UKF and the results are displayed in Figure 11. It is assumed that the data on the SRF-PLL and the FD channels are contaminated by outliers with a magnitude of 0.1 p.u. from $t = 3$ s to $t = 3.49$ s and from $t = 3.51$ s to $t = 4$ s, respectively. As seen in Figure 11, the GM-UKF can provide a reliable and accurate estimation, resulting in better damping of the frequency oscillations.

Let us now analyze the ability of the Fusion-UKF and the fusion GM-UKF to deal with a noise following a thick tailed probability distribution. Figure 12 displays the instantaneous mean squared errors of the state estimation methods considering that the measurement noise follows four distributions,

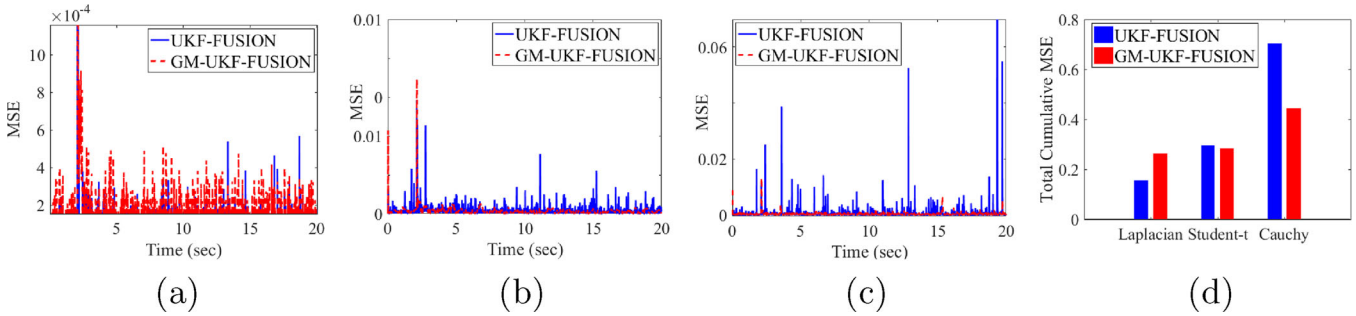

FIGURE 12 Performance of the fusion estimation methods against noise following non-Gaussian probability distributions: (a) Laplace noise distribution with mean 0 and standard deviation 0.0003 p.u.; (b) Student-t distribution with two degrees of freedom and with mean 0 and standard deviation 0.0006 p.u.; (c) Cauchy distribution with the location parameter $a = 0$ and the scale parameter $b = 0.0003$; and (d) frequency total cumulative mean squared errors for three noise probability distributions.

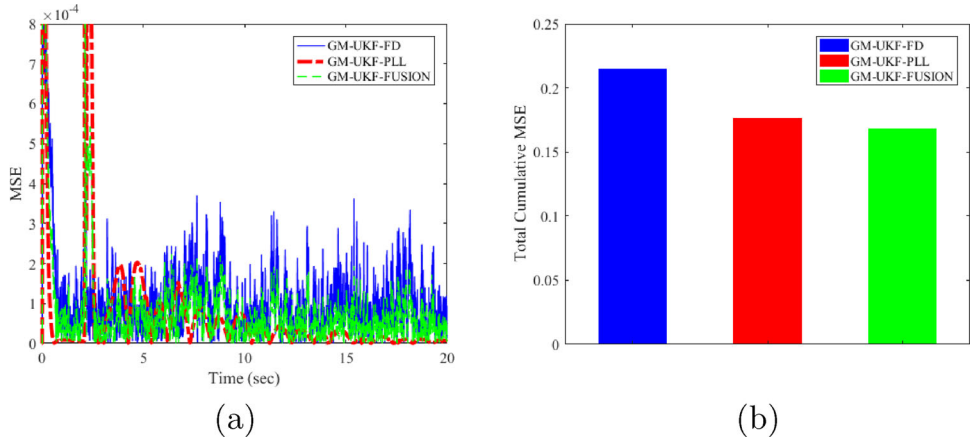

FIGURE 13 Comparison of the frequency estimation using the fusion GM-UKF, the GM-UKF-FD, and the GM-UKF-PLL. The noise on the FD follows the Cauchy distribution with the location parameter $a = 0$ and the scale parameter $b = 0.0003$ while the noise on the PLL follows the Gaussian distribution: (a) mean squared errors of the frequency estimation; (b) total frequency cumulative mean squared errors.

namely, (1) a Gaussian distribution, (2) a Laplace distribution, (3) a Student's t-distribution, and (4) a Cauchy distribution. The results show that the Fusion-UKF performs satisfactory for a noise following the Gaussian and the Laplace distribution while the fusion GM-UKF performs better for a noise following thicker tailed distributions such as the Student-t distribution with a low degree of freedom and the Cauchy distribution.

Now, let us compare the Fusion GM-UKF, which makes use of both measurements, with the GM-UKF presented in [23]. We refer to the latter as the GM-UKF-FD. For a more comprehensive study, we also consider the so-called GM-UKF-PLL, which only processes SRF-PLL measurements. Note that in [23], only the FD calculations are employed. Figure 13 compares the performances of the fusion GM-UKF, the GM-UKF-FD, and the GM-UKF-PLL. For a better assessment of the Fusion GM-UKF effect, we assume that the noise on the FD follows the Cauchy distribution with a location parameter of $a = 0$ and a scale parameter of $b = 0.0003$ and that the noise on the PLL follows the Gaussian distribution with the previously assumed parameters. Figures 13a and 13b display the mean squared errors and the total cumulative mean squared errors of the three estimation methods when they estimate the frequency on the local Bus 10. The overall outcome of this comparison is that the fusion approach has increased the efficiency and robustness of the frequency estimation method even more than the GM-UKF-FD presented in [23]. The first reason is the statistical enhancement that the covariance intersection approach provides to the frequency estimation. The other and more important reason is the higher outlier detection ability provided by the projection statistics to the redundant SRF-PLL measurements. In fact, even if the SRF-PLL measurements are not quite precise, they still can play a role in increasing the probability of the outlier detection technique.

Let us now analyze the impact of the delays on the received FD and SRF-PLL signals. Figure 14 presents the state estimation results of the bus frequency when two signals are not of the same time benchmark. As noticed, the fusion GM-UKF enjoys the highest estimation performance when there are delays on the FD measurements. It can also handle missing measurements. To show that, let us assume that the measurements on both channels are missed between $t = 3$ s and $t = 4$ s and the last received measurements in $t = 2.99$ s are used as the only

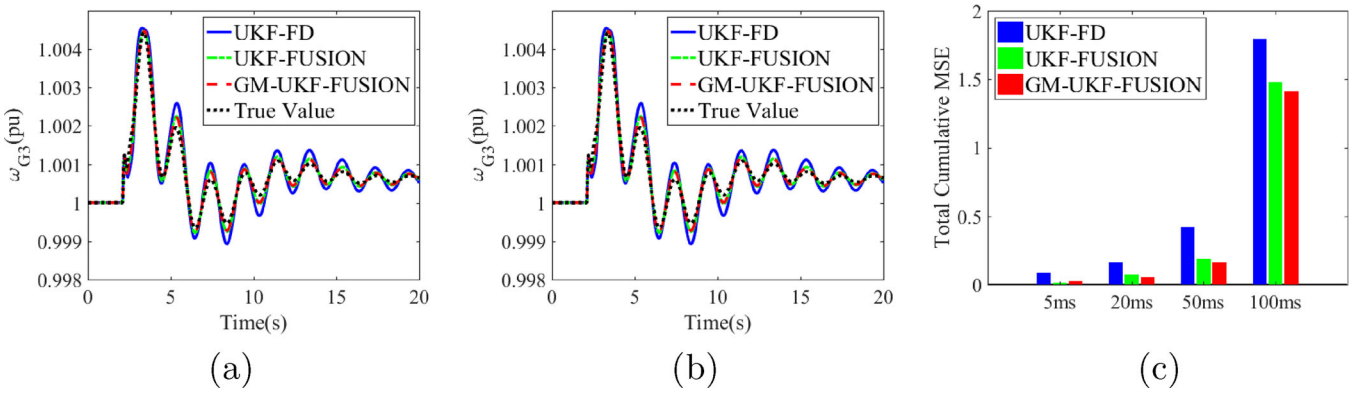

FIGURE 14 Performance of the fusion estimation methods against delay differences between the SRF-PLL and the FD signals: (a) comparison of the performance of the UKF-FD, the UKF-PLL, and the Fusion-UKF for delay=50 ms; (b) effect of the time delay on the damping of the frequency oscillations of *G*3; (c) mean squared errors of the frequency estimation methods for different delays.

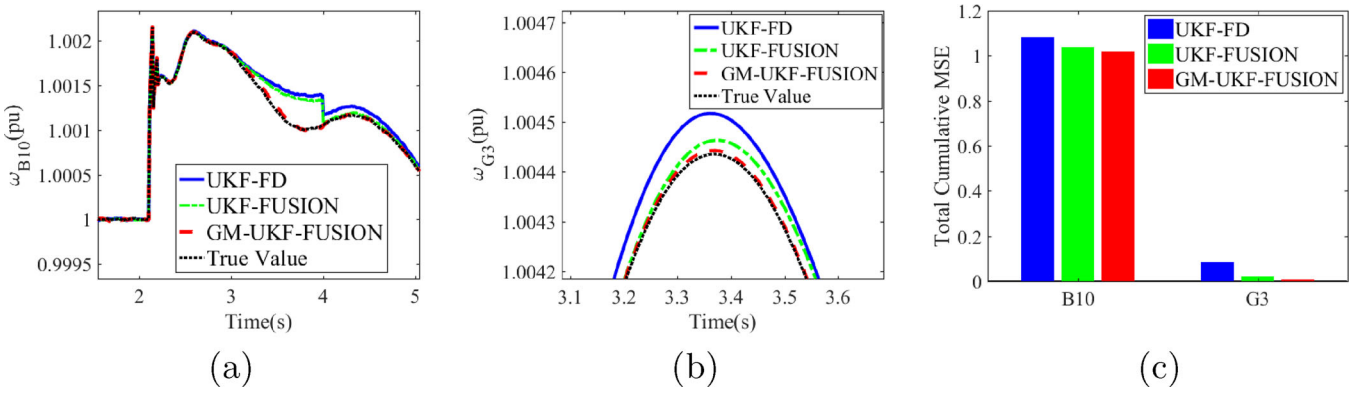

FIGURE 15 Performance of the fusion estimation of the frequency estimation at Bus 10 and its effect on improving frequency oscillation damping of Generator G3 by the WAPSS with missing data between $t = 3$ s to $t = 4$ s: (a) frequency estimation at Bus 10; (b) frequency oscillation damping of Generator G3; and (c) total mean squared errors of the oscillation damping estimation.

available information in the next time interval. Figure 15 displays the results on the performance of the fusion GM-UKF in this situation. As seen, it provides the best performance as compared to the other methods.

4.4 | fusion GM-UKF estimation for other faults/load shedding scenarios

As another important evaluation of the Fusion GM-UKF estimation and its effect on the frequency oscillation damping, we apply other types of disturbances on the line between Buses 3 and 101 at time $t = 2.1$ s. These disturbances are: (1) a line-to-ground fault; (2) a two-line-to-ground fault; (3) a line-to-line fault; and (4) a loss-of-line leading to a setpoint change. We also apply a fifth disturbance that consists in a 20-percent loss of loads on Bus 4 starting from $t = 2.1$ s. The results are displayed in Figure 16. Here, outliers are included among the SRF-PLL data from $t = 3$ s to $t = 3.49$ s and among the FD data from $t = 3.5$ s to $t = 4$ s. It is observed that the fusion method is able to provide the feedback signal of a higher quality for the WAPSS, leading to an improved frequency oscillation damping.

4.5 | Performance of the fusion GM-UKF frequency estimation in new-england test system

We carry out a study on frequency estimation within the 39-Bus New-England power system, whose data are provided in [9]. Zhang and Bose [9] study inter-area oscillations in that system and recommend to install a WAPSS on Generator *G*7. The latter takes the frequency at Bus 16 as its feedback signal. As in the previous example, it is assumed that a SRF-PLL is located at Bus 16, which calculates the angular frequency at that bus and sends it to the fusion processing center. Also, the angular frequencies of all the generators are simultaneously estimated in a decentralized manner and are sent to the fusion center. In the fusion center, after carrying out a centralized estimation and fusion, the high-quality estimate of frequency at Bus 16 is applied to WAPSS installed on Generator *G*7. A 3-phase fault is assumed to happen on the line between Buses 1 and 39 at $t = 2.1$ s. The fault is then removed at $t = 2.15$ s from Bus 1and at $t = 2.20$ s from 39.

To show the effectiveness of the fusion GM-UKF method, it is assumed that the FD data is contaminated by observation

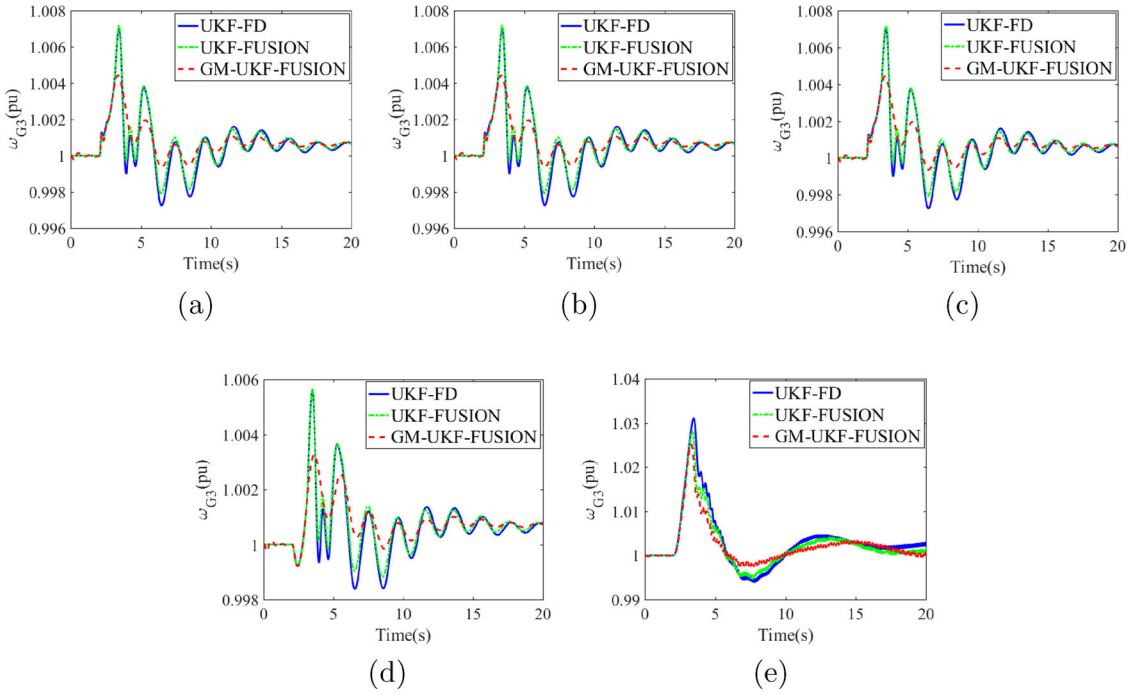

FIGURE 16 The ability of the fusion GM-UKF to improve the frequency oscillation damping by the WAPSS against various disturbances at $t = 2.1s$, which includes: (a) a line-to-ground fault on Line 3-101; (b) a two-line-to-ground fault on the same line; (c) a line-to-line fault; (d) a line outage leading to a setpoint change; and (e) a 20 percent loss-of-load at Bus 4.

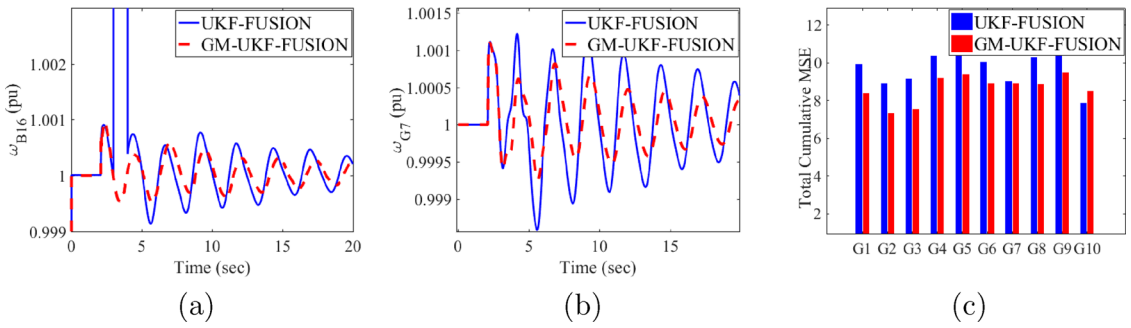

FIGURE 17 Estimation performed at Bus 16 in the New England test system by the fusion filters when there are outliers among the FD data from $t = 3$ s to $t = 4$ s using the Fusion-UKF and the fusion GM-UKF; (a) the impact of outliers on the frequency estimations at Bus 16; (b) the impact of outliers on the damping of the frequency oscillations of Generator $G7$; (c) comparison of the MSEs of the Fusion-UKF and of the fusion GM-UKF for all the generators.

outliers of 0.1 p.u. from $t = 3s$ to $t = 4s$. Figure 17a displays the results of the angular frequency estimation at Bus 16. The effect of the robust frequency estimation on the WAPSS frequency stabilization is shown in Figure 17b. As seen, the fusion GM-UKF provides an accurate estimation at the time where the outlier is applied, but the Fusion-UKF dos not since it tracks the outlier. This leads to better stabilization when using the fusion GM-UKF estimations as the feedback signal rather than using the Fusion-UKF. Figure 17c displays the MSEs. As for Table 2, it provides the simulation times of all the tested algorithms. As seen from Table 2 and the previously presented figures, the fusion GM-UKF algorithm provides lower estimation error with higher computing time. The run-time of the filtering method is a limitation especially for very large networks calling for fast processors. This can be regarded as the price to pay to have higher robustness against non-Gaussian noises and outliers. Note that the proposed fusion UKF has reasonable computational speed and may be used most of times when no outliers exist.

5 | CONCLUSIONS

To construct a high quality feedback signal for the WAPSS, the Fusion-UKF is adapted based on the time dependent weighting on the signals provided by the SRF-PLL and the FD

TABLE 2 Comparison of the simulation times (in seconds) for all the tested algorithms.

Algorithms	Two-area Case	New England case
GM-UKF-Fusion	39	98
GM-UKF-FD	37	95
GM-UKF-PLL	32	89
UKF-Fusion	29	76
UKF-FD	27	74
UKF-PLL	24	72

calculations. Furthermore, to address the problem of outliers among the data, a robust fusion GM-UKF has been developed with a modified calculation of the weights based on the projection statistics. The results show that the latter is able to improve the performance of the frequency damping. Moreover, it enhances the quality of the feedback data when there are outliers among the data provided by the SRF-PLL and the FD.

AUTHOR CONTRIBUTIONS

Ali Farahani: Investigation, software, writing - original draft. Amir Abolmasoumi: Conceptualization, formal analysis, methodology, resources, software, supervision, writing - review and editing. Lamine Mili: Conceptualization, supervision, writing - review and editing. Mohammad Bayat: Resources, supervision, validation.

CONFLICT OF INTEREST STATEMENT

The authors have declared no conflict of interest.

FUNDING INFORMATION

There is no funding to declare regarding this manuscript.

DATA AVAILABILITY STATEMENT

Data available on request from the corresponding author.

ORCID

Amir H. Abolmasoumi https://orcid.org/0000-0001-9739-1340

Mohammad Bayat https://orcid.org/0000-0003-1465-0015

REFERENCES

1. Klein, M., Rogers, G.J., Kundur, P.: A fundamental study of inter-area oscillations in power systems. IEEE Trans. Power Syst. 6(3), 914–921 (1991)
2. Kundur, P.: Power System Stability and Control. In: EPRI Power System Engineering Series. McGraw-Hill, New York (1994)
3. Rogers, G.: Power system oscillations. In: Power Electronics and Power Systems. Springer, New York (2012)
4. Tzounas, G., Liu, M., Murad, M.A.A., Milano, F.: Impact of realistic bus frequency measurements on wide-area power system stabilizers. In: 2019 IEEE Milan PowerTech, pp. 1–6. IEEE, Piscataway (2019)
5. Abolmasoumi, A.H., Moradi, M.: Nonlinear ts fuzzy stabilizer design for power systems including random loads and static synchronous compensator. international transactions on electrical energy systems. IEEE Trans. Power Syst. 28(4), 1559–1564 (2018)
6. Mohanty, A.K., Barik, A.K.: Power system stability improvement using facts devices. Int. J. Modern Eng. Res. 1(2), 666–672 (2011)
7. Chow, J.H., Sanchez-Gasca, J.J., Ren, H., Wang, S.: Power system damping controller design-using multiple input signals. IEEE Control Syst. Mag. 20(4), 82–90 (2000)
8. Aboul-Ela, M.E., Sallam, A.A., McCalley, J.D., Fouad, A.A.: Damping controller design for power system oscillations using global signals. IEEE Trans. Power Syst. 11(2), 767–773 (1996)
9. Zhang, Y., Bose, A.: Design of wide-area damping controllers for interarea oscillations. IEEE Trans. Power Syst. 23(3), 1136–1143 (2008). https://doi.org/10.1109/TPWRS.2008.926718
10. Shakarami, M.R., Faraji Davoudkhani, I.: Wide-area power system stabilizer design based on grey wolf optimization algorithm considering the time delay. Electr. Power Syst. Res. 133, 149–159 (2016)
11. Chung, C.Y., Wang, K.W., Tse, C.T., Bian, X.Y., David, A.K.: Probabilistic eigenvalue sensitivity analysis and pss design in multimachine systems. IEEE Trans. Power Syst. 18(4), 1439–1445 (2003)
12. Zhang, P., Messina, A.R., Coorick, A., Cory, B.J.: Selection of locations and input signals for multiple svc damping controllers in large scale power systems. In: IEEE Power Engineering Society 1999 Winter Meeting (Cat. No.99CH36233), vol. 1, pp. 667–670. IEEE, Piscataway (1999)
13. Heniche, A., Kamwa, I.: Assessment of two methods to select wide-area signals for power system damping control. IEEE Trans. Power Syst. 23(2), 572–581 (2008)
14. Song, F.F., Bi, T.S., Yang, Q.X.: Study on wide area measurement system based transient stability control for power system. In: 2005 International Power Engineering Conference, vol. 2, pp. 757–760. IEEE, Piscataway (2005)
15. Zhao, J., Zhang, G., La Scala, M.: A two-stage robust power system state estimation method with unknown measurement noise. In: 2016 IEEE Power and Energy Society General Meeting (PESGM), pp. 1–5. IEEE, Piscataway (2016)
16. Zhou, N., Meng, D., Huang, Z., Welch, G.: Dynamic state estimation of a synchronous machine using pmu data: A comparative study. IEEE Trans. Smart Grid 6(1), 450–460 (2014)
17. Zhao, J., Gómez-Expósito, A., Netto, M., Mili, L., Abur, A., Terzija, V., Kamwa, I., Pal, B., Singh, A. K., Qi, J., et al.: Power system dynamic state estimation: Motivations, definitions, methodologies, and future work. IEEE Trans. Power Syst. 34(4), 3188–3198 (2019)
18. Chen, J., Dou, C., Xiao, L., Wang, Z.: Fusion state estimation for power systems under dos attacks: A switched system approach. IEEE Trans. Syst. Man Cybern. Syst. 49(8), 1679–1687 (2019)
19. Singh, A.K., Pal, B.C.: Decentralized robust dynamic state estimation in power systems using instrument transformers. IEEE Trans. Signal Process. 66(6), 1541–1550 (2018)
20. Mir, A.S., Singh, A.K., Senroy, N.: Robust observer based methodology for frequency and rate of change of frequency estimation in power systems. IEEE Trans. Power Syst. 36(6), 5385–5395 (2021)
21. Chen, X., Henry, M., Duncan, S.R.: An enhanced algorithm for frequency estimation in power systems. In: 2018 UKACC 12th International Conference on Control (CONTROL), pp. 140–145. IEEE, Piscataway (2018)
22. Milano, F., Ortega, A.: Frequency divider. IEEE Trans. Power Syst. 32(2), 1493–1501 (2017)
23. Zhao, J., Mili, L., Milano, F.: Robust frequency divider for power system online monitoring and control. IEEE Trans. Power Syst. 33(4), 4414–4423 (2018)
24. Ortega, A., Milano, F.: Comparison of different pll implementations for frequency estimation and control. In: 2018 18th International Conference on Harmonics and Quality of Power (ICHQP), pp. 1–6. IEEE, Piscataway (2018)
25. Freijedo, F.D., Doval-Gandoy, J., Lopez, O., Acha, E.: Tuning of phase-locked loops for power converters under distorted utility conditions. IEEE Trans. Ind. Appl. 45(6), 2039–2047 (2009)
26. Zhao, J., Zhang, G., La-Scala, M., Wang, Z.: Enhanced robustness of state estimator to bad data processing through multi-innovation analysis. IEEE Trans. Ind. Inf. 13(4), 1610–1619 (2016)

27. Zhao, C., Topcu, U., Low, S.H.: Optimal load control via frequency measurement and neighborhood area communication. IEEE Trans. Power Syst. 28(4), 3576–3587 (2013)
28. Huang, C., Li, F., Zhan, L., Xu, Y., Hu, Q., Zhou, D., Liu, Y.: Data quality issues for synchrophasor applications part ii: problem formulation and potential solutions. J. Mod. Power Syst. Clean Energy 4(3), 353–361 (2016)
29. Huang, C., Li, F., Zhou, D., Guo, J., Pan, Z., Liu, Y., Liu, Y.: Data quality issues for synchrophasor applications part i: A review. J. Mod. Power Syst. Clean Energy 4(3), 342–352 (2016)
30. Liu, Y., Gracia, J.R., Ewing, P.D., Zhao, J., Tan, J., Wu, L., Zhan, L.: Impact of measurement error on synchrophasor applications. Oak Ridge National Lab. (ORNL), Oak Ridge, TN (2015)
31. Sundararajan, A., Khan, T., Moghadasi, A., Sarwat, A.I.: Survey on synchrophasor data quality and cybersecurity challenges, and evaluation of their interdependencies. J. Mod. Power Syst. Clean Energy 7(3), 449–467 (2019)
32. Ortega, A., Milano, F.: Comparison of different pll implementations for frequency estimation and control. In: 2018 18th International Conference on Harmonics and Quality of Power (ICHQP), pp. 1–6. IEEE, Piscataway (2018)
33. Gandhi, M.A., Mili, L.: Robust kalman filter based on a generalized maximum-likelihood-type estimator. IEEE Trans. Signal Process. 58(5), 2509–2520 (2010)
34. Zhao, J., Mili, L.: A robust generalized-maximum likelihood inscented kalman filter for power system dynamic state estimation. IEEE J. Sel. Top. Signal Process. 12(4), 578–592 (2018)
35. Zhao, J., Mili, L.: Robust unscented kalman filter for power system dynamic state estimation with unknown noise statistics. IEEE Trans. Smart Grid 10(2), 1215–1224 (2019)
36. Zhao, J., Netto, M., Mili, L.: A robust iterated extended kalman filter for power system dynamic state estimation. IEEE Trans. Power Syst. 32(4), 3205–3216 (2017). https://doi.org/10.1109/TPWRS.2016.2628344
37. Ortega, A., Milano, F.: Comparison of bus frequency estimators for power system transient stability analysis. 2016 IEEE International Conference on Power System Technology (POWERCON), pp. 1–6. IEEE, Piscataway (2016)
38. Farahani, A., Abolmasoumi, A.H., Bayat, M., Mili, L.: A fast outlier-robust fusion estimator for local bus frequency estimation in power systems. In: 2020 10th Smart Grid Conference (SGC), pp. 1–6. IEEE, Piscataway (2020)
39. Farahani, A., Abolmasoumi, A.H., Bayat, M.: Fusion estimation of local bus frequency for robust wide area power system stabilizer. In: 2021 7th International Conference on Control, Instrumentation and Automation (ICCIA), pp. 1–5. IEEE, Piscataway (2021)
40. Aboul-Ela, M.E., Sallam, A., McCalley, J.D., Fouad, A.: Damping controller design for power system oscillations using global signals. IEEE Trans. Power Syst. 11(2), 767–773 (1996)
41. Yao, W., Jiang, L., Wu, Q., Wen, J., Cheng, S.: Delay-dependent stability analysis of the power system with a wide-area damping controller embedded. IEEE Trans. Power Syst. 26(1), 233–240 (2010)
42. Wang, Y., Yemula, P., Bose, A.: Decentralized communication and control systems for power system operation. IEEE Trans. Smart Grid 6(2), 885–893 (2014)
43. Ortega, A., Milano, F.: Impact of frequency estimation for vsc-based devices with primary frequency control. In: 2017 IEEE PES Innovative Smart Grid Technologies Conference Europe (ISGT-Europe), pp. 1–6. IEEE, Piscataway (2017)
44. Liggins, M., Hall, D., Llinas, J.: Handbook of Multi Sensor Data Fusion: Theory and Practice. In: Electrical Engineering & Applied Signal Processing Series, 2nd ed. CRC Press, Boca Raton, FL (2017)
45. Raol, J.R.: Multi-Sensor Data Fusion with MATLAB. CRC Press, Boca Raton, FL (2009)
46. Uhlmann, J.K.: Dynamic Map Building and Localization: New Theoretical Foundations. University of Oxford, Oxford (1995)
47. Chen, L., Arambel, P.O., Mehra, R.K.: Estimation under unknown correlation: Covariance intersection revisited. IEEE Trans. Autom. Control 47(11), 1879–1882 (2002)
48. Julier, S.J., Uhlmann, J.K.: Using covariance intersection for slam. Rob. Auton. Syst. 55(1), 3–20 (2007)
49. Donoho, D.L., Gasko, M.: Breakdown properties of location estimates based on halfspace depth and projected outlyingness. Ann. Statist. 20(4), 1803–1827 (1992). https://doi.org/10.1214/aos/1176348890
50. Mili, L., Cheniae, M.G., Vichare, N.S., Rousseeuw, P.J.: Robust state estimation based on projection statistics [of power systems]. IEEE Trans. Power Syst. 11(2), 1118–1127 (1996)
51. Chow, J.H., Cheung, K.W.: A toolbox for power system dynamics and control engineering education and research. IEEE Trans. Power Syst. 7(4), 1559–1564 (1992)

How to cite this article: Farahani, A., Abolmasoumi, A.H., Mili, L., Bayat, M.: A robust fusion bus frequency estimation method to improve frequency oscillation damping in power systems. IET Gener. Transm. Distrib. 17, 4172–4187 (2023).
https://doi.org/10.1049/gtd2.12976